ORGANIC PROCESS RESEARCH & DEVELOPMENT
OPR&D

Full Paper

Development of a Robust and Reusable Microreactor Employing Laser Based Mid-IR Chemical Imaging for the Automated Quantification of Reaction Kinetics

Hakan Keles, Flavien Susanne, Hamish Livingstone, Sarah Hunter, Charles Wade, Rose Emily Bourdon, and Andrew Rutter

Org. Process Res. Dev., **Just Accepted Manuscript** • DOI: 10.1021/acs.oprd.7b00245 • Publication Date (Web): 13 Oct 2017

Just Accepted

ACS Publications

Organic Process Research & Development is published by the American Chemical Society. 1155 Sixteenth Street N.W., Washington, DC 20036

Development of a Robust and Reusable Microreactor Employing Laser Based Mid-IR Chemical Imaging for the Automated Quantification of Reaction Kinetics

Hakan Keles[a,*], Flavien Susanne[b], Hamish Livingstone[c], Sarah Hunter[b], Charles Wade[d], Rose Bourdon[a], Andrew Rutter[b].

[a] Research and Development, GlaxoSmithKline, Gunnels Wood Road, Stevenage SG1 2NY, U.K.
[b] Product and Process Engineering, GlaxoSmithKline, Gunnels Wood Road, Stevenage SG1 2NY, U.K.
[c] Technical Development, Glaxo Wellcome Manufacturing Pte Ltd 1, Pioneer Sector 1, Singapore, 628413
[d] Global API Chemistry, GlaxoSmithKline, Gunnels Wood Road, Stevenage SG1 2NY, U.K.

* Corresponding author.

Tel.: +44 (0)143 876 2711

E-mail address: hakan.x.keles@gsk.com

For Table of Contents Only

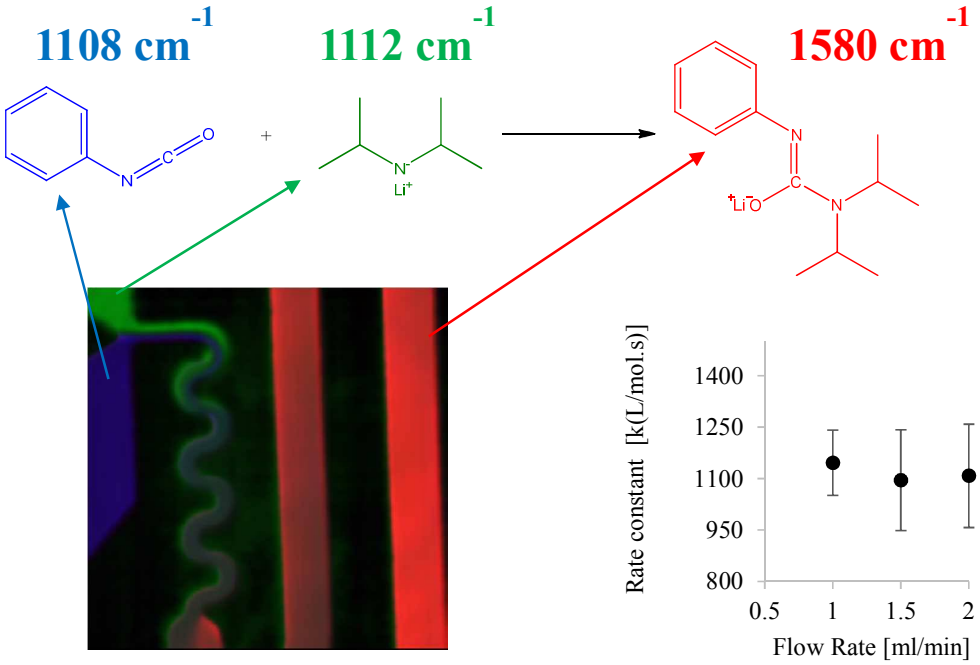

Abstract

A robust, reusable microreactor coupled with laser based mid-IR chemical imaging and automated analysis is reported, for the first time, with its application to monitor and quantify a fast organometallic chemistry in flow. We have investigated the sub-second organometallic addition reaction between lithium diisopropylamide and phenyl isocyanate in order to define and tune microfluidic system parameters such as residence time using physical system constraints (flow rate, reactor volume) to aid process development. Selectivity of mid-IR video rate capture of the flow response of reactants and product enabled the qualitative assessment of mixing properties. Furthermore, we report a minimally supervised automated image analysis toolbox that generates concentration as a function of residence time enabling the calculation of reaction rate constant, *k*, using hyperspectral data cubes. Finally, we report the reproducibility of quantification precision by measuring the rate constant, at 3 different flow rates with 3 replicates for each flow rate. These findings show the potential value of the micro-reactor particularly when coupled with automated mid-IR transmission analysis for the study of flow chemistry at the micron scale, assisting in the understanding of the reaction kinetics and mixing properties and enhancing the value of the chemical imaging based, automated quantification of microfluidics.

Keywords;

Microfluidics, QCL, Kinetics, Flow chemistry.

1 Introduction

Continuous processing is a manufacturing methodology that dominates the high volume production, often associated with refining and petrochemical manufacture. On the other hand, Active Pharmaceutical Ingredient (API) manufacture is a low volume, high value product, where demand is uncertain. Therefore, API manufacture had traditionally been in the domain of batch manufacture, which remains the mainstay of the pharmaceutical industry.

However, in the past decade there has been a growing interest in the application of continuous processing, or flow chemistry, in the pharmaceutical industry for two reasons. Firstly, flow chemistry enables a diversity of reactions from which to synthesize a molecule[1-2]. Such approaches facilitate a simpler synthetic route to a molecule that may in turn produce a simpler manufacturing process[1]. Secondly, a rationale has emerged based around factory or supply chain benefit. This approach argues that telescoping multiple synthetic steps together in a continuous supply chain leads to benefits including reducing inventories and allowing more responsiveness to product demand[3].

The difficulty with this approach is that it is not trivial to design multistep synthetic routes as it requires solving interlinked chemical and engineering problems. To address the design problem of performing a coupled synthesis, our team has been invested in augmenting the experimental design process. This involved sequencing together mechanistic process models of the unit operations to accelerate understanding of how chemistry is linked from one stage to another. This requires obtaining process rates such as main and side reaction rates and mixing times early in the design process for the main and side reactions where the availability of material is restricted. Understanding the mechanistic role that mixing of reactants play in continuous manufacture of APIs is key to tune the manufacturing parameters to a high and sustained level in a desired time-frame. Further mechanistic models should enable better operation decisions, for example how process changes impact product quality by linking the model to the control system.

Current practice for obtaining kinetic data relies on batch time-course experimentation coupled with in-line (eg. reaction calorimetry, UV, FT-IR or Raman) and offline (eg. HPLC, GC) analytical techniques[4-7]. Although the batch model is well established for facilitating most types of experiments, it is not best suited to relatively fast (sub-second) flow experiments which form a significant proportion of reactions carried out in flow in pharmaceutical portfolios[8]. Alternatively, mesoreactors (mm size devices) are used, facilitating relatively fast reactions by increased mixing efficiency[9-10]. Such devices, however, are often difficult to couple with *in-situ* analytics and require larger quantities of starting materials and reagents to run[10]. In contrast, rapid development in micro-reaction technology (spatially resolved micron sized features in a closed volume) has led to a variety of available micromixers and using microfluidics to generate kinetic data has become an established practice. Stopped flow reactors, often coupled with UV/visible spectrophotometry, conductometry and/or fluorometric detection are commonly used for generating kinetic data[11]. However such techniques can be limited by the rate of data acquisition. In addition, significantly fast reactions can achieve completion within the system dead time with instruments providing no online visibility of the mixing zone[11]. Similarly, continuous flow devices which correspond positioning in the system to time, offer the advantage of easily providing multiple data points for each time point, again, coupled with varying detection techniques including inline quench[5], thermal imaging[12] conversely, however, generation of multiple time points using these devices requires multiple detection points and can result in significant material consumption. Furthermore, microfluidic mixers are often sealed and can be blocked during use and are also difficult to couple with in-line process analytical technologies (PAT) due to their size[10]. Therefore, robust, reusable and flexible microfluidic devices coupled with fast, *in-situ*, label-free and spatially resolved

chemical probing, preferably with automated analysis, is highly desirable.

Since the successful coupling of microfluidic devices with spatially resolved chemical probing is key if one needs to optimise reaction kinetics in micro-flow, fluorescence microscopy has been frequently used facilitating single molecule probing with high sensitivity[13-14]. More recently, direct methods (i.e. not requiring a label or dye) such as Fourier Transform Infrared (FT-IR) spectroscopic imaging[15], spatially resolved Raman spectroscopy[5] and, in particular, Raman microscopy[16] have facilitated the monitoring of reaction kinetics and has been reported with increasing frequency. Today, FT-IR modality also remains a popular choice for chemical imaging, however, for transmission measurements, the shallow penetration depth of the infrared phonons emitted from a globar source limits its application, particularly for aqueous systems and speed of image collection still remains in the minute domain making it difficult to track sub-second reactions for a wavelength of interest. On the other hand, Raman microscopy does not suffer from aqueous interference due to the weak Raman scatting property of the water molecule and recently it has become faster with the use of Electron Multiplying Charged Coupled Device (EMCCD) detectors, facilitating collection of a few thousands of pixels, each containing a full Raman spectrum, in approximately a second[17]. However, when imaging mm sized domains containing tens of thousands of pixels within microfluidics, practically, compulsory mechanical movement potentially perturbs the fast chemistry in flow and requirement of dark environment during acquisition minimises visual access to micro-reactors. Furthermore, to acquire from a few mm scale field of view with less than a 10 micron pixel size and sufficient signal to noise ratio (SNR) (achieved at the cost of increased number of spectral accumulation, multiplying total acquisition time), which is necessary to resolve sub 100 micron features, Raman microscopy, even with the fast detectors, still remains to be relatively slow[18]. On the other hand, nonlinear Raman microscopy, also commercially available, facilitates best selectivity, sensitivity and spatial resolution at video rate per wavelength without modifying the sample. However, slow laser tuning (~10 minutes for 50 wavelengths) and fine focus depth makes it less suitable for imaging aforementioned millimetric devices rapidly, although it is better suited for nanoscale probing, in comparison to conventional Raman microscopy[19]. In contrast, although still with relatively poorer spatial resolution than Raman microscopy, with the comparatively recent commercial introduction of tunable Quantum Cascade Laser (QCL) based IR spectrometers coupled with un-cooled bolometer detectors, dispersive transmission and transflection mid-infrared imaging is facilitated with reported advantages over FT-IR imaging[20]. Specifically, the higher flux QCL source of the microscope compared to the conventional globar source of FT-IR microscopes facilitate better SNR and wider field of view for the same pixel size[21-22]. In addition, the use of a laser based dispersive mid-IR instrument at a discrete wavelength can allow for the collection of spatially resolved images at video rate (30 ms per frame) that is not possible with a FT-IR instrument[23]. The relatively high spectral power density of the QCLs, in comparison to globar sources, facilitates a deeper penetration depth allowing for collection of transmission mid-IR spectra with relatively good SNR at 100 μm through most solvents[24].

As previously mentioned, the mixing time is a key parameter for any microfluidic mixer. The sub-millisecond mixing of biomolecular reactions has been reported, and more recently using transmission mid-IR hyperspectral imaging through a 75 μm path length, comparing the mixer performance to predictions from a simulation[25]. Similarly, B. Lendl *et al* have developed a fast mixing microfluidic device coupled with fast infrared measurements[26].

One area which also shows promise in the field of microfluidics is their application to chemistry involving highly reactive and hazardous organometallic reagents, frequently used in the production of many organic, pharmaceutical intermediates. The obvious advantage of high heat transfer enables more efficient processing of these exothermic chemistries[27-28],

there are, however, few reports of using this reaction technology to enable process understanding and development in a robust (up to 11 bar pressure, ~50 ºC temperature, almost insoluble in most organic solvents and acids) microreactor coupled with analytical technology allowing for the automated elucidation of important attributes. Furthermore, it is desirable for the reactor to be economic and easy to clean to overcome the risk of blockages that often form in the channels due to using air and water sensitive organometallic reagents.
We report the development of a robust and reusable microreactor coupled with a QCL based mid-IR microscope demonstrating the *in-situ* monitoring of a sub-second chemical reaction in flow, followed by quantification of the reaction rate constant using custom built automated software (graphical user interface), for the first time. Moreover, this technique enhances reaction pathway and kinetic understanding in flow chemistry applications

2 Experimental

2.1 Materials

All materials were purchased from Sigma Aldrich and kept in a nitrogen environment once containers were opened. Solutions of lithium diisopropylamide (LDA), (product number 361798, CAS number 4111-54-0) and phenyl isocyanate (product number 78750, CAS number 103-71-9) were both prepared to 0.25 M in dry tetrahydrofuran (THF), (product number 401757, CAS number 109-99-9).

2.2 Design and Development of Reusable Microfluidic Reactors Utilizing Mid-IR Detection

As mentioned previously mid-IR microscopy is a label-free method which images structures or chemical reagents by displaying their individual, intrinsic molecular vibrations. However, in transmission mode samples need to be introduced to the mid-IR path length on or between mid-IR transparent materials. CaF_2 is one of the most suitable substrates to use as it transmits well between the so called mid-IR fingerprint region of 900-1800 cm^{-1} and is also almost insoluble in most organic materials and acids. Inert (chemical and high temperature resistant) diamond wafers could be used, however, CaF_2 is more economical and sufficient (stable up to ~50 ºC) for studying the organic chemical reaction reported here.
A custom flow cell holder, as shown in Figure 1A, was designed in two parts from stainless steel and used four screws outfitted with metal stamps to provide an adequate clamping force on the flow cell. This feature allows the cell to be easily reused. The overall outer dimensions of the assembly as can be seen in scale view in Figure 1A, are 45 mm in diameter and ~17 mm in height. Each holder consists of a 5 mm hole, enabling infrared and visible light transmission through CaF_2 windows. As shown in Figure 1B, a polytetrafluoroethylene (PTFE) gasket is sandwiched between two circular, polished CaF_2 windows (4 mm x 25 mm). The top CaF_2 window is undrilled and the bottom window consists of 4 x 0.5 mm holes. Each CaF_2 window sits on top of a flat circular seal which aids alignment and reduces the likelihood of fracture during clamping. A removable connector sits in the bottom holder, which contains the previously mentioned seal. The connector and seal each have 4 holes corresponding to the holes in the drilled CaF_2 window. Inlet and outlet tubing passes through four holes in the side of the bottom holder into a recess in the underside, allowing for the introduction of solutions in to the CaF_2 constrained PTFE channels. In this case, as can be seen in Figure 1D, only two inlets and one outlet were used. Precise laser cutting of the channels in the 100 µm thick PTFE film facilitates custom mixing geometries based on user requirement. The microreactor design went through 3 iterations until all required parameters were optimised and was made as a bespoke order by Dolomite Ltd. Royston, UK.

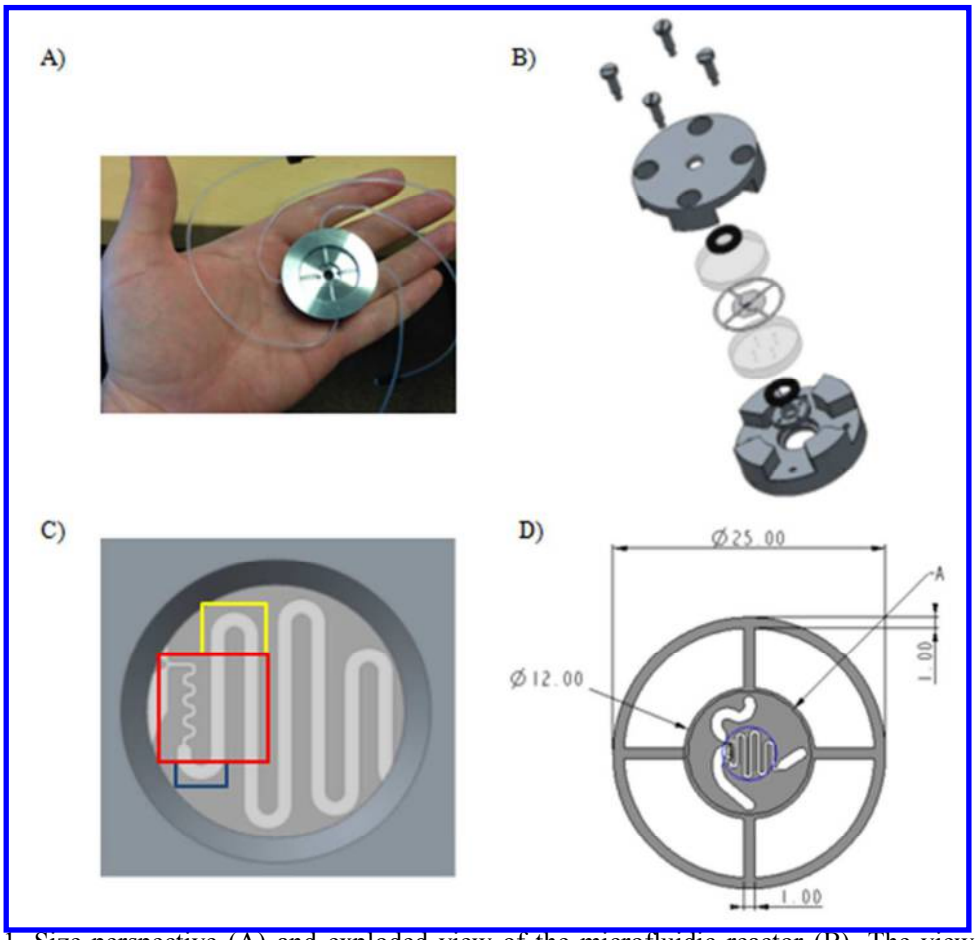

Figure 1. Size perspective (A) and exploded view of the microfluidic reactor (B). The view of the microfluidic channels when placed in the flow cell holder, the region of interest selected to monitor using the mid-IR microscope and the two bends in the channel that are not seen in the forthcoming hyperspectral images, as indicated with a red, blue and yellow frame accordingly (C). Schematic of the PTFE gasket, where the blue circle indicates the visible section of the gasket when placed in the flow cell holder (D).

In this case, the flow design consisted of 2 parts, a serpentine mixing zone and a residence channel, such that adequate mixing of the reaction mixture was ensured and mass transfer limitations to the rate of reaction were prevented. The experimental Villermaux-Dushman reaction scheme[29] was used and the interaction by exchange with the mean (IEM) mixing model was used to quantify mixing performance following the protocol outlined by Reckamp *et. al.*[30]. Using the chip design, shown in Figure 1, with a serpentine channel with dimensions of 100 µm depth and width at a combined flow rate of 1 ml/min, it was estimated that mixing time would equal residence time after 4 bends. By keeping the combined flow rate of the reaction mixture equal to 1 ml/min, and above, the mixing performance of the serpentine channel was therefore assured. This mixing property of the microreactor was readily possible to assess using mid-IR hyperspectral imaging.

The channel features of the PTFE gasket visible through the 5 mm window are shown in Figure 1C. However, this is not indicative of the field of view from the mid-IR microscope, as the maximum field of view per image is limited to 2 x 2 mm^2, as shown in the red square. The gasket, outlined in Figure 1D, has a diameter of 25 mm, is 100 µm deep and consists of 1 mm wide inlet and outlet channels, a 100 µm wide serpentine mixer and a 300 µm wide, 23

mm long residence channel.
The system contains no active temperature control yet however thermal mass of the process media as well as the chip have been considered to establish a heat balance model and ensure isothermicity for the chemistry reported herein.

2.3 Flow Setup

A precision syringe pump (Pump 11 Elite, Harvard Apparatus) outfitted with 2 x 10 mL plastic syringes (Luer lock, NORM-JECT) was used to introduce dry THF and solutions of LDA and phenyl isocyanate into the microfluidic device via two inlets. The syringe pump was calibrated to deliver flow rates of 0.5, 0.75 and 1 ml/min, to give combined flow rates of 1, 1.5 and 2 ml/min, respectively.

2.4 QCL Based Mid-IR Imaging

QCL based mid-IR imaging was performed in transmission mode using a Spero (Daylight Solutions Inc., CA, US) microscope that was equipped with 4 individual QCLs facilitating continuous coverage of the 900–1800 cm^{-1} wavenumber range with 4 wavenumbers spectral and 4.25 x 4.25 μm^2 lateral pixel size within a 2 x 2 mm^2 field of view using a 4.0X (0.15 NA) magnification IR objective coupled with a 480 x 480 bolometer detector. A laser calibration curve was collected through an 8 mm thick CaF_2 window material (Crystan Ltd, UK) in order to normalise laser intensity across the aforementioned mid-IR collection range for all intensities. A new calibration curve was collected and used before each of the experiments reported herein, in order to minimise effect of laser drift on SNR. After the laser calibration, hyperspectral images were collected in transmission mode and ratioed against a background collected from the same field of view of the same samples but including the solvent (THF in this case) within the micro channels.

3 Results and Discussion

The use of microreactors is becoming an increasingly common method to study fast, difficult to control reactions[31-32]. The inherent low volumes used by microreactors provide not only economic advantages due to minimal use of reagents but also increased safety when using hazardous, highly reactive reagents such as organometallic materials[9, 33]. Although highly reactive, these reagents are commonly used in the synthesis of organic compounds by forming carbon-carbon bonds[34] or acting as strong bases[35], for example. We have developed an analytical method combining flow chemistry in a microreactor with laser based mid-IR imaging followed by the automated analysis of reaction kinetics.
Using our method, we have studied the reaction between the organometallic reagent, LDA, and phenyl isocyanate *in-situ* during flow. The reaction scheme outlined in Figure 2 shows the nucleophilic addition of LDA to phenyl isocyanate to produce a lithium salt product.

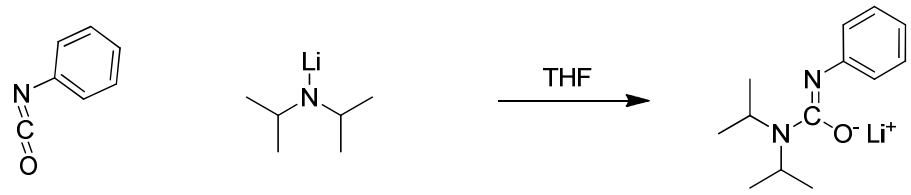

Figure 2. Reaction scheme. Nucleophilic addition to phenyl isocyanate using lithium diisopropylamide.

Although LDA is typically considered to be a poor nucleophile due to significant steric

hindrance; the lack of acidic protons on phenyl isocyanate and the previously mentioned fast mixing of the microreactor meant that addition of LDA to the isocyanate group occurred in less than a second. Such fast reaction requires even faster data capture in order to monitor kinetics reproducibly at a wavelength of interest. Laser based mid-IR imaging facilitated the generation of chemical images in an area of interest using a commercially available dispersive microscope, in ~30 ms per wavenumber. Each pixel of the focal plane array (FPA) bolometer detector acts as an individual infrared detector, allowing the simultaneous collection of multiple mid-IR transmission spectra. A stack of 2D images can be collected within ~5 minutes covering the full mid-IR fingerprint region, or in seconds covering a sparser region of interest proving good temporal resolution and SNR[23].

Focussing on a 2 x 2 mm^2 area within the microreactor (including the two inlets, the serpentine mixer and the pathway thereafter) mid-IR microscopy facilitated the simultaneous collection of hundreds of reagent and product spectra each extracted from a single 4.25 μm^2 pixel, from a single experiment in flow.

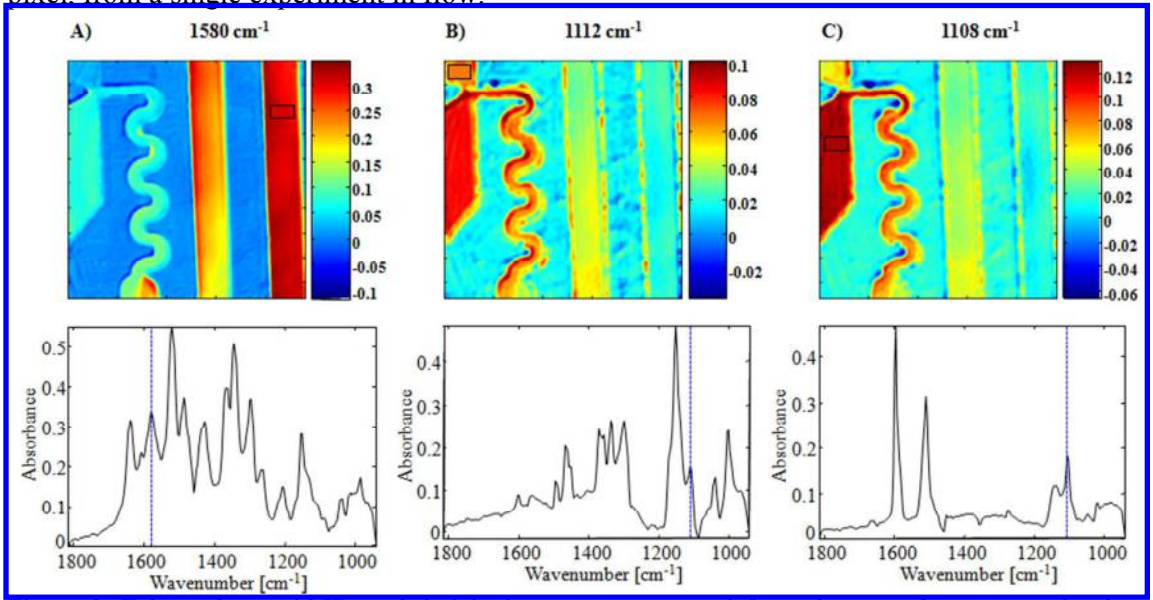

Figure 3. False colour mid-IR peak height images, as extracted from the same hyperspectral cube, (top) of the lithium salt product (1580 cm^{-1}), LDA (1112 cm^{-1}) and phenyl isocyanate (1108 cm^{-1}) and averaged spectra (below) from the black box (30 x 45 pixels) indicated in the former, shown in A, B and C, respectively.

By selecting the wavenumber of interest available within a mid-IR hyperspectral image cube, absorbance values directly proportional to concentration of the different species therein can be spatially resolved. Figure 3 shows image frames selected from the same hyperspectral image in this manner. During the reaction outlined in Figure 2, at a 1.5 ml/min combined flow rate of the two reactants, unprocessed peak height images of the lithium salt product, LDA and phenyl isocyanate are shown in Figure 3 as A, B and C respectively. Under each image in Figure 3, averaged spectra of each component extracted from the black rectangle indicated in each image, can be seen.

For the nucleophilic reaction shown in Figure 2, characteristic mid-IR vibrational spectroscopic bands of 1112 cm^{-1} representing the anti-symmetric stretch of C-N (ν_{as}(C-N))[36], 1108 cm^{-1} representing the symmetric stretch of N=C=O (ν_s(N=C=O))[37] and 1580 cm^{-1}, representing the stretching vibration of C=C-C (ν(C=C-C))[38] were determined for LDA, phenyl isocyanate and the lithium salt product, respectively. It is important to note that mid-IR hyperspectral images often require pre-processing and deconvolution and therefore, a variance based multivariate deconvolution such as multivariate curve resolution or curve fitting would potentially facilitate complete separation of reactants and product and would

potentially improve resolution and contrast in the images and accuracy of relative quantification using them[39]. However, a number of factors, as can be seen in spectra presented in Figure 3, including inherent mid-IR selectivity of the system (facilitated by discrete, intense Lorentzian shaped peaks) and unremarkable baseline distortion, univariate analysis using raw absorbance values was seen to readily facilitate an adequate qualitative separation between species with minimal effort.

The increasing level of red colour after the serpentine mixing zone indicates product formation along the microchannel at 1580 cm^{-1} as shown in Figure 3A. Similarly, the consumption of the reagents LDA (1112 cm^{-1}) and phenyl isocyanate (1108 cm^{-1}) can be qualified by the decreasing levels of red colour, as seen in Figure 3B and C, respectively.

As previously discussed for the chip design, it was expected that for combined flow rates of ≥1 ml/min, the mixing time would be less than the residence time of the serpentine ensuring that the reactants were homogenously mixed as they left the serpentine. Mid-IR imaging has also enabled the monitoring of this phenomenon. This is demonstrated qualitatively in Figure 3, where the reactants are consumed and the product starts forming at the end of the serpentine mixer.

The rate constant, k, is an important kinetic parameter that links the rate of a chemical reaction to the concentration of its reactants and is conventionally determined by means of manual calculations requiring multiple sets of data. Therefore, automation of this process is highly desirable in order to save the scientist time and materials during process optimisation. In Figure 3B and C, the decrease in absorbance for the reactants LDA and phenyl isocyanate, respectively, as a function of residence time along the microchannel (respective to the inlets), can clearly be seen. Consequently, by converting the distance of the microchannel into residence time using Equation 1,

$$\tau = \frac{V}{Q} \quad \textbf{Equation 1}$$

(where τ is residence time, V is channel volume, and Q is the flow rate) and by using the concentration values calculated via calibration curves for each of the reactants (Figure S 3), the reaction rate constant, k was calculated. The calibration curves were obtained from six known concentrations for each reagent, where absorbance data was collected from the same microreactor under the same conditions.

In order to facilitate high throughput analysis of multiple reactions under changing parameters, a bespoke toolbox was developed in MATLAB (R2016a) that only requires a user defined path, combined flow rate, pixel size and channel dimensions to be inputted. These variables can be saved and re-used for subsequent repeat flow experiments. The path consisted of a succession of "nodes", and quantitatively shows the change in absorbance at specific wavenumbers, as a function of time. The interface of the toolbox, where an example path has been defined, can be seen in Figure 4. The toolbox automates the calculation of cumulative distance along the path and combines this with the aforementioned user-inputted parameters, for the calculation of residence time. It should be noted that due to the field of view of 2 x 2 mm^2, the two bends of the microchannel as indicated in Figure 1C in yellow and blue frames, cannot be seen in the hyperspectral images indicated in the red frame. However, the path length used in the residence time calculation included the assumed Euclidean distance for these two bends based on their size. The tool box was designed so that these custom parameters could be also added manually. The linear equations from the aforementioned reactant calibration curves were inputted into the toolbox to convert mid-IR absorbance to concentration. The interface of the results window relative to the run outlined in Figure 4 is shown in Figure S 1.

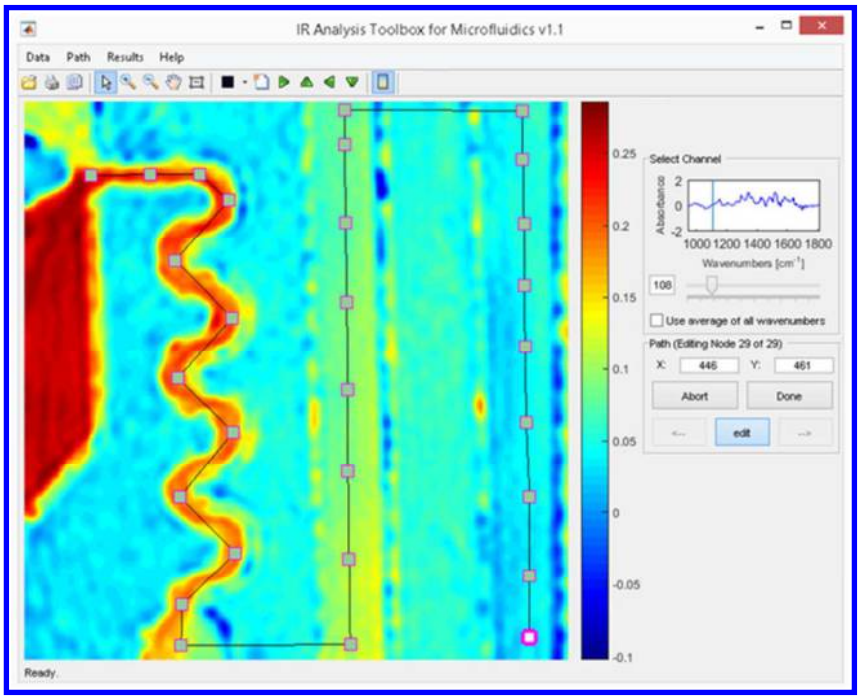

Figure 4. A snapshot of the graphical user interface (GUI) of the toolbox, showing a jet colour mid-IR hyperspectral image of a 480 x 480 pixels (2 x 2 mm^2) section of the microreactor at 1108 cm^{-1}, demonstrating the consumption of phenyl isocyanate as a function of time along the chip. The user defined path consists of a series of 9 x 9 pixel averaged areas (nodes) at the specified wavenumber. The hyperspectral image was taken from a different run than that seen in Figure 3.

The data generated, change in reactant and/or product concentration as a function of residence time, using the image analysis toolbox, facilitates the calculation of kinetic parameters, such as the reaction rate constant.

As mentioned previously, although the use of mid-IR compatible, bespoke flow cells have been reported[18, 21, 26], there has been a lack of demonstration in reproducibility and automated quantification of kinetic parameters requiring a robust, reusable microreactor. To address not only this, but also to demonstrate the application of the method developed for an industrially relevant flow chemistry, we have studied the organometallic addition reaction shown in Figure 2 as demonstrated in Figure 3 for 1.5 ml/min combined flow rate and at two additional combined flow rates of 1 and 2 ml/min, shown in Figure 5. Subsequently, we have compared the calculated reaction rate constants to assess robustness of the experimental setup.

Three repeats were conducted at each flow rate, using the same microreactor 9 times, successively, to assess the reproducibility of the system described. Figure 5 shows the formation of product as a function of residence time, for the 3 combined flow rates of 1, 1.5 and 2 ml/min shown in A, B and C, respectively, analoguos to that of Figure 3A.

In Figure 5, a small discrepancy is seen between colour scales, mainly due to a change in SNR caused by expected laser drift and a change in water vapour levels between time-solved images ratioed against the same, previously collected THF background. Despite this small discrepancy, Figure 5 qualitatively demonstrates that the product formation occurs later in the microchannel, proportional to increasing combined flow rates of 1, 1.5 and 2 ml/min in Figure 5 A, B and C respectively. This is expected as flow rate is inversely proportional to residence time (Equation 1).

The rate of the reaction is independent of flow rate and is a function of the concentration of

reactants and temperature (Equations 2 and 3, where A is the Arrhenius constant, E_A is the activation energy, R is the gas constant and T is the temperature), assumed to have remained constant during the flow experiments.

$$Rate = k[LDA][Phenyl\ Isocyanate]$$ **Equation 2**

$$k = Ae^{-\frac{(E_A)}{(RT)}}$$ **Equation 3**

As defined in Equation 3, the rate constant, is also independent of the flow rate and was therefore used to assess the robustness of the method in that triplicate experiments conducted at three different flow rates would produce the same k value.

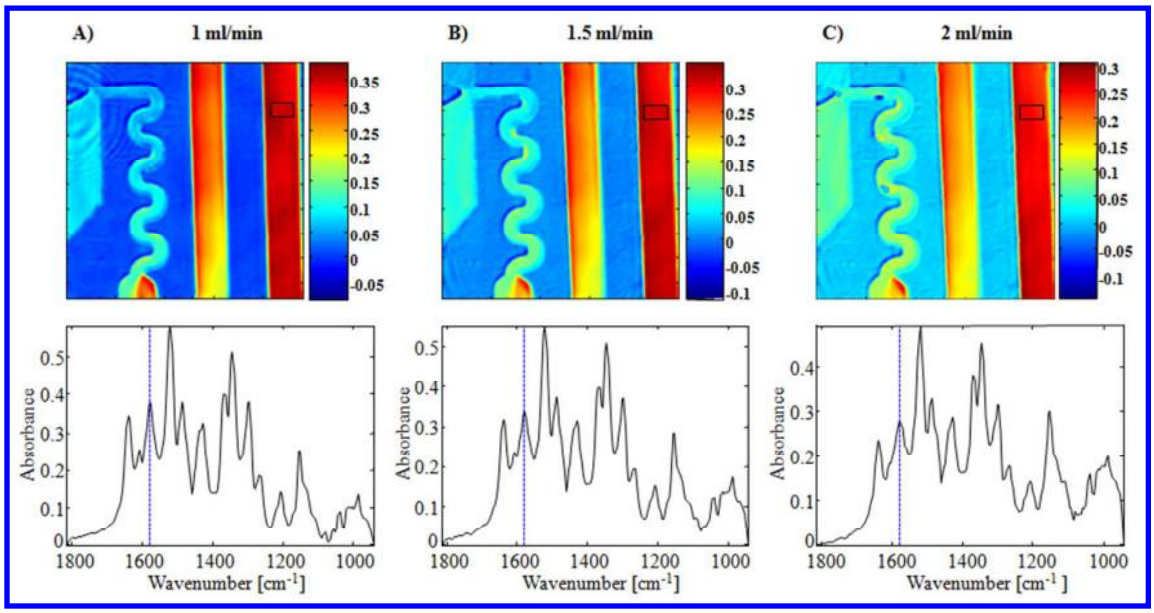

Figure 5. False colour mid-IR peak height (1580 cm^{-1}) images of the product (top) and corresponding averaged spectra (below) from the black box (30 x 45 pixels), as indicated in the former as a function of flow rate of 1, 1.5 and 2 ml/min, in (A), (B) and (C) respectively.

The reaction rate constant can be calculated either based on the rate of formation of product, or the rate of consumption of a single reactant, if the mass balance is known. As it can be seen in Figure 3, both rates of product formation and reactant consumption were readily available as spatially resolved mid-IR absorbance values. However, in this case, it was not possible to isolate the product to obtain a calibration curve and therefore, the rate constant was calculated for each of the 9 experiments based on the concentration decrease of both reactants as extracted from the MATLAB based toolbox, as previously described. This calculation was perfomed using DynoChem 2011 (Scale-up Systems Limited) software.
DynoChem creates a kinetic model using user defined values and parameters and finds the best fit of this model to experimental data by means of minimising the sum of squared residuals[40].
Calculated rate constants from triplicate experiments conducted at combined flow rates of 1, 1.5 and 2 ml/min are listed in Table 1.

Table 1. Rate constants from triplicate experiments conducted at flow rates of 1, 1.5 and 2 ml/min. The errors are determined by DynoChem software within a 95% confidence interval.

Combined Flow Rate [ml/min]	Run 1 (k [L/mol.s])	Run 2 (k [L/mol.s])	Run 3 (k [L/mol.s])
1	1151 ± 94	1238 ± 79	1146 ± 95
1.5	1252 ± 89	1131 ± 182	1095 ± 147
2	1293 ± 172	1187 ± 146	1108 ± 151

Owing to the rate constant's independence to flow rate, as described by Equations 2 and 3, it can be seen in Table 1 that the errors reported are assumed to be reliable in comparing reproducibility of the experiment reported, mainly in that the reaction rate constant doesn't significantly change proportionally to flow rate nor with number of repeats. The respective rate constant for each of the 9 experiments (average reaction rate =1178±128) reported are seen to lie between each of the associated errors of the other 8 experiments. These errors were calculated by DynoChem, within a 95% confidence interval between the software's model and the experimental data.

As indicated from Table 1, it can clearly be seen that our demonstrated approach of combining the use of a laser based mid-IR microscope with a robust, reusable microreactor and latterly with a series of automated analytical software tools, was successful in extracting reproducible, industrially relevant kinetic information. However it should also be noted that this is a relative comparison between controlled runs therefore the *k* values are not absolute but to facilitate investigation of measurement robustness. Furthermore, as mentioned previously, the system has no active temperature control yet and the calibration and mixing experiments were conducted at room temperature assuming there was enough heat sink with in the chip. The reproducibility of *k* values listed in Table 1 and consistent peak positions that can be observed in Figure 5 between consecutive runs at varying flow rate have also proved this assumption for the micro reactor considering the reaction reported.

4 Conclusions

A detailed overview of the development of a robust and reusable microreactor utilising spatially resolved laser based mid-IR chemical detection and automated analysis is reported. The method was applied to real-time monitoring of organometallic chemistry in continuous flow; demonstrating the ability to quantify concentration profiles during sub-second flow reactions, using the automated data processing procedure for the first time.

Our approach is demonstrated to be a successful method in monitoring, *in-situ*, the reaction of LDA with Phenyl Isocyanate. Utilising the chemical selectivity of the transmission mid-infrared methodology reported, reactant concentration profiles, analogous to those obtained using standard FT-IR flow equipment have been obtained for the reaction subjected to a range of flow rates. Performing direct measurements at different locations in the microreactor resulted in obtaining kinetic characteristics of the design rapidly, thus facilitating increase in the experimental throughput.

The hyperspectral images resulting from this experimental approach were analysed using a custom made automated analytical software tool, enabling the extraction of the industrially important rate constant. Furthermore, the calculation of the rate constant over 9 experiments was shown to be consistent, demonstrating the reproducibility and the accuracy of the method reported.

This platform is demonstrated to be powerful in speed and selectivity for reactants and

product(s), offering a great potential in both the chemical development and scale-up activities. Thus, this combination of techniques has enabled kinetic evaluation of flow systems and offered a material and time-efficient solution in process development. Current work includes catalytic reaction monitoring and implementation of temperature control of the microreactor in order to quantify temperature effect on reaction kinetics.

Acknowledgements

The authors would like to thank Roger Barrett and Jason Williams for chemistry, Albert Ziegler for toolbox discussions.

Supporting Information

Additional information from the automated analysis toolbox and detailed conversion procedure of mid-IR absorbance data to concentration using reactant calibration curves is provided in supplementary information section.

5 References

1. Wiles, C.; Watts, P., Continuous flow reactors: a perspective. *Green Chemistry* **2012,** *14* (1), 38-54.
2. Malet-Sanz, L.; Susanne, F., Continuous flow synthesis. A pharma perspective. *J. Med. Chem* **2012,** *55* (9), 4062-4098.
3. Strang, D. Pharma 2020: Supplying The Future. Which path will you take? https://www.pwc.com/gx/en/pharma-life-sciences/pdf/pharma-2020-supplying-the-future.pdf (accessed 5/5/2017).
4. Moore, J. S.; Jensen, K. F., Batch Kinetics in Flow: Online IR Analysis and Continuous Control. *Angewandte Chemie* **2013,** *53* (2), 470-473.
5. Schwolow, S.; Braun, F.; Rädle, M.; Kockmann, N.; Röder, T., Fast and Efficient Acquisition of Kinetic Data in Microreactors Using In-Line Raman Analysis. *Organic Process Research & Development* **2015,** *19* (9).
6. Benito-Lopez, F.; Verboom, W.; Kakuta, M.; Gardeniers, J. H. G. E.; Egberink, R. J. M.; Oosterbroek, E. R.; Bergb, A. v. d.; Reinhoudt, D. N., Optical fiber-based on-line UV/Vis spectroscopic monitoring of chemical reaction kinetics under high pressure in a capillary microreactor. *Chemical Communications* **2005,** (22), 2857-2859.
7. Keybl, J.; Jensen, K. F., Microreactor System for High-Pressure Continuous Flow Homogeneous Catalysis Measurements. *Industrial & Engineering Chemistry Research* **2011,** *50* (19), 11013-11022.
8. Yoshida, J.-i., *Flash chemistry: fast organic synthesis in microsystems*. John Wiley & Sons: 2008.
9. Mason, B. P.; Price, K. E.; Steinbacher, J. L.; Bogdan, A. R.; Mcquade, D. T., Greener Approaches to Organic Synthesis Using Microreactor Technology. *Chemical Reviews* **2007,** *107* (6), 2300-2318.
10. Elvira, K. S.; i Solvas, X. C.; Wootton, R. C. R.; deMello, A. J., The past, present and potential for microfluidic reactor technology in chemical synthesis. *Nat Chem* **2013,** *5* (11), 905-915.
11. Clarke, R. J.; Khalid, M. A. A., Pumps, Channels, and Transporters - Methods of Functional Analysis. John Wiley & Sons.: New Jersey, 2015; pp 179-209.
12. Zhang, J. S.; Zhang, C. Y.; Lui, G. T.; Luo, G. S., Measuring enthalpy of fast exothermal reaction with infrared thermography in a microreactor. *Chemical Engineering Journal* **2016,** *295*, 384-390.
13. Matthews, S. M.; Elder, A. D.; Yunus, K.; Kaminski, C. F.; Brennan, C. M.; Fisher, A. C., Quantitative kinetic analysis in a microfluidic device using frequency-domain fluorescence lifetime imaging. *Analytical chemistry* **2007,** *79* (11), 4101-4109.
14. Tsuchiya, N.; Kuwabara, K.; Hidaka, A.; Oda, K.; Katayama, K., Reaction kinetics of dye decomposition processes monitored inside a photocatalytic microreactor. *Physical Chemistry Chemical Physics* **2012,** *14* (14), 4734-4741.
15. Polshin, E.; Verbruggen, B.; Witters, D.; Sels, B.; De Vos, D.; Nicolaï, B.; Lammertyn, J., Integration of microfluidics and FT-IR microscopy for label-free study of enzyme kinetics. *Sensors and Actuators B: Chemical* **2014,** *196*, 175-182.
16. Chrimes, A. F.; Khoshmanesh, K.; Stoddart, P. R.; Mitchell, A.; Kalantar-zadeh, K., Microfluidics and Raman microscopy: current applications and future challenges. *Chemical Society Reviews* **2013,** *42* (13), 5880-5906.
17. Qi, J.; Li, J.; Shih, W.-C., High-speed hyperspectral Raman imaging for label-free compositional microanalysis. *Biomedical Optics Express* **2013,** *4* (11), 2376-2382.
18. Salzer, R.; Siesler, H. W., *Infrared and Raman Spectroscopic Imaging*. 2nd ed.; Wiley-VCH: Weinheim, Germany 2014.
19. Cheng, J.-X.; Xie, X. S., *Coherent Raman Scattering Microscopy*. 2nd ed.; CRC Press FL, USA, 2017.
20. Kole, M. R.; Reddy, R. K.; Schulmerich, M. V.; Gelber, M. K.; Bhargava, R., Discrete Frequency Infrared Microspectroscopy and Imaging with a Tunable Quantum Cascade Laser. In *Analytical Chemistry*, American Chemical

Society: 2012; Vol. 84, pp 10366-10372.
21. Yeh, K.; Kenkel, S.; Liu, J.-N.; Bhargava, R., Fast infrared chemical imaging with a quantum cascade laser. *Analytical chemistry* **2014,** *87* (1), 485-493.
22. Schwaighofer, A.; Alcaráz, M. R.; Araman, C.; Goicoechea, H.; Lendl, B., External cavity-quantum cascade laser infrared spectroscopy for secondary structure analysis of proteins at low concentrations. *Scientific Reports* **2016,** *6*, 33556.
23. Childs, D. T. D.; Hogg, R. A.; Revin, D. G.; Rehman, I. U.; Cockburn, J. W.; Matcher, S. J., Sensitivity Advantage of QCL Tunable-Laser Mid-Infrared Spectroscopy Over FTIR Spectroscopy. *Applied Spectroscopy Reviews* **2015,** *50* (10), 822-839.
24. Lendl, B.; Frank, J.; Schindler, R.; Müller, A.; Beck, M.; Faist, J., Mid-Infrared Quantum Cascade Lasers for Flow Injection Analysis. *Analytical Chemistry* **2000,** *72* (7), 1645-1648.
25. Kise, D. P.; Magana, D.; Reddish, M. J.; Dyer, R. B., Submillisecond mixing in a continuous-flow, microfluidic mixer utilizing mid-infrared hyperspectral imaging detection. *Lab on a Chip* **2014,** *14* (3), 584-591.
26. Buchegger, W.; Wagner, C.; Lendl, B.; Kraft, M.; Vellekoop, M. J., A highly uniform lamination micromixer with wedge shaped inlet channels for time resolved infrared spectroscopy. *Microfluidics and Nanofluidics* **2011,** *10* (4), 889-897.
27. Laue, S.; Haverkamp, V.; Mleczko, L., Experience with Scale-Up of Low-Temperature Organometallic Reactions in Continuous Flow. *Organic Process Research & Development* **2016,** *20* (2), 480-486.
28. Hafner, A.; Filipponi, P.; Piccioni, L.; Meisenbach, M.; Schenkel, B.; Venturoni, F.; Sedelmeier, J., A Simple Scale-up Strategy for Organolithium Chemistry in Flow Mode: From Feasibility to Kilogram Quantities. *Organic Process Research & Development* **2016,** *20* (10), 1833-1837.
29. Commenge, J.-M.; Falk, L., Villermaux–Dushman protocol for experimental characterization of micromixers. *Chemical Engineering and Processing: Process Intensification* **2011,** *50* (10), 979-990.
30. Reckamp, J.; Bindels, A.; Duffield, S.; Liu, Y. C.; Bradford, E.; Ricci, E.; Susanne, F.; Rutter, A., Mixing Performance Evaluation for Commercially Available Micromixers Using Villermaux-Dushman Reaction Scheme with the Interaction by Exchange with the Mean Model. *Organic Process Research & Development* **2017,** *21*, 816-820.
31. Yoshida, J.-i.; Takahashi, Y.; Nagaki, A., Flash chemistry: flow chemistry that cannot be done in batch. *Chemical communications* **2013,** *49* (85), 9896-9904.
32. Noël, T.; Su, Y.; Hessel, V., Beyond Organometallic Flow Chemistry: The Principles Behind the Use of Continuous-Flow Reactors for Synthesis In *Organometallic Flow Chemistry*, Noël, T., Ed. Springer International Publishing: Switzerland, 2015; p 2.
33. de Mello, A.; Wootton, R., FOCUS But what is it good for? Applications of microreactor technology for the fine chemical industry. *Lab on a Chip* **2002,** *2* (1), 7N-13N.
34. Shinokubo, H.; Oshima, K., Transition Metal‐Catalyzed Carbon− Carbon Bond Formation with Grignard Reagents− Novel Reactions with a Classic Reagent. *European Journal of Organic Chemistry* **2004,** *2004* (10), 2081-2091.
35. Collum, D. B.; McNeil, A. J.; Ramirez, A., Lithium diisopropylamide: Solution kinetics and implications for organic synthesis. *Angewandte Chemie International Edition* **2007,** *46* (17), 3002-3017.
36. Piasek, Z.; Urbanski, T., The infra-red absorption spectrum and structure of urea. *B Pol Acad Sci-Tech X* **1962**, 113-120.
37. Ham, N.; Willis, J., The vibrational spectra of organic isothiocyanates. *Spectrochimica Acta* **1960,** *16* (3), 279-301.
38. Coates, J., Interpretation of infrared spectra, a practical approach. *Encyclopedia of analytical chemistry* **2000**, 10815-10837.
39. Keles, H.; Naylor, A.; Clegg, F.; Sammon, C., The application of non-linear curve fitting routines to the analysis of mid-infrared images obtained from single polymeric microparticles. *Analyst* **2014,** *139* (10), 2355-2369.
40. Bright, R.; Dale, D. J.; Dunn, P. J.; Hussain, F.; Kang, Y.; Mason, C.; Mitchell, J. C.; Snowden, M. J., Identification of New Catalysts to Promote Imidazolide Couplings and Optimisation of Reaction Conditions Using Kinetic Modelling. *Organic Process Research & Development* **2004,** *8* (6), 1054-1058.